Fabrication of an inexpensive, implantable cooling device for reversible brain deactivation in animals ranging from rodents to primates

Dylan F. Cooke, Adam B. Goldring, Itsukyo Yamayoshi, Phillippos Tsourkas, Gregg H. Recanzone, Alex Tiriac, Tingrui Pan, Scott I. Simon and Leah Krubitzer

J Neurophysiol 107:3543-3558, 2012. First published 7 March 2012;
doi: 10.1152/jn.01101.2011

J Neurophysiol 107: 3543–3558, 2012.
First published March 7, 2012; doi:10.1152/jn.01101.2011.

Fabrication of an inexpensive, implantable cooling device for reversible brain deactivation in animals ranging from rodents to primates

Dylan F. Cooke,[1] Adam B. Goldring,[1,2] Itsukyo Yamayoshi,[3] Phillippos Tsourkas,[3] Gregg H. Recanzone,[1,4] Alex Tiriac,[1] Tingrui Pan,[3] Scott I. Simon,[3] and Leah Krubitzer[1,2]

[1]*Center for Neuroscience, University of California, Davis, California;* [2]*Department of Psychology, University of California, Davis, California;* [3]*Department of Biomedical Engineering, University of California, Davis, California; and* [4]*Department of Neurobiology, Physiology and Behavior, University of California, Davis, California*

Submitted 2 December 2011; accepted in final form 4 March 2012

Cooke DF, Goldring AB, Yamayoshi I, Tsourkas P, Recanzone GH, Tiriac A, Pan T, Simon SI, Krubitzer L. Fabrication of an inexpensive, implantable cooling device for reversible brain deactivation in animals ranging from rodents to primates. *J Neurophysiol* 107: 3543–3558, 2012. First published March 7, 2012; doi:10.1152/jn.01101.2011.—We have developed a compact and lightweight microfluidic cooling device to reversibly deactivate one or more areas of the neocortex to examine its functional macrocircuitry as well as behavioral and cortical plasticity. The device, which we term the "cooling chip," consists of thin silicone tubing (through which chilled ethanol is circulated) embedded in mechanically compliant polydimethylsiloxane (PDMS). PDMS is tailored to compact device dimensions (as small as 21 mm^3) that precisely accommodate the geometry of the targeted cortical area. The biocompatible design makes it suitable for both acute preparations and chronic implantation for long-term behavioral studies. The cooling chip accommodates an in-cortex microthermocouple measuring local cortical temperature. A microelectrode may be used to record simultaneous neural responses at the same location. Cortex temperature is controlled by computer regulation of the coolant flow, which can achieve a localized cortical temperature drop from 37 to 20°C in less than 3 min and maintain target temperature to within ±0.3°C indefinitely. Here we describe cooling chip fabrication and performance in mediating cessation of neural signaling in acute preparations of rodents, ferrets, and primates.

cryoloop; inactivation; plasticity; magnetic resonance compatible; cortex; biocompatible

MUCH OF WHAT IS KNOWN about brain function and plasticity derives from the study of traumatic and experimental lesions to discreet portions of a cortical macrocircuit. An example is the early work of Mishkin and colleagues (Mishkin 1979, 1982; Mishkin and Ungerleider 1982; Ungerleider and Mishkin 1982). Their studies of monkeys with lesions in specific portions of visual cortex clearly revealed how the brain processes different subclasses of inputs and established the ideas of hierarchical processing in the visual system and the two streams of visual information processing. Unfortunately, removal of cortical tissue permanently alters the region of interest and ultimately not only affects the area ablated but also can lead to retrograde degeneration of connected cortical areas and subcortical nuclei, leading to permanent changes in the entire network. While interesting in and of itself, such plasticity can confound the study of the ablated region's normal function (e.g., Padberg et al. 2010). For this reason, reversible deactivation through cooling or injection of chemicals is valuable for providing important insights into how normal circuits function in real time.

Chemical deactivation, for example, the use of muscimol or cobalt chloride, has been used effectively in a wide range of studies of brain function (see Malpeli 1999 for review). Compared with cooling, such techniques are especially useful for deactivating deep structures or very small volumes of tissue. Other requirements, however, such as repeated deactivation on shorter time scales, favor cooling. Deactivation and restoration of normal activity can be accomplished faster and more consistently with cooling, because chemical deactivation involves continuous diffusion and metabolization of the drug. Consequently, the volume of deactivation constantly changes and can be hard to reproduce precisely on subsequent deactivation sessions. See Lomber (1999) for a comparison of cooling and chemical deactivation.

Compared with permanent and reversible chemical deactivation, previously utilized heat exchange devices have distinct advantages and disadvantages. Early devices used chilled circulating alcohol (e.g., Skinner and Lindsley 1968) or Freon evaporation (e.g., Benita and Conde 1972) to reduce cortical activity, but the devices were difficult to construct, and in-cortex electrodes and/or thermocouples were used mainly in acute preparations. Since then, a variety of cooling devices have been developed and applied by several groups (Clarey et al. 1996; Clemo and Stein 1986; Fuster and Alexander 1970; Fuster and Bauer 1974; Girard et al. 1992, 1991; Horel 1996; Horel et al. 1984; Michalski et al. 1993, 1994; Sandell and Schiller 1982; Schiller and Malpeli 1977; Sherk 1978; Shindy et al. 1994; Zhang et al. 1986). These devices were used to study a variety of different cortical areas, for example, to examine the effects of deactivation of a particular area on the neural responses of other areas or on behavior. In most cases these devices were relatively large, sometimes covering half of a large field or several cortical fields (e.g., Alexander and Fuster 1973; Girard et al. 1992; Horel 1996; Sandell and Schiller 1982; Schiller and Malpeli 1977). Some of the devices were also limited to a particular shape (e.g., circular), rather than tailored to the shape of the cortical area of interest, and many did not contain an in-cortex microthermocouple. Perhaps because of these limitations, to our knowledge, many of these devices are no longer in use.

A more recent device based on Peltier thermoelectric cooling has been applied to study epilepsy (Imoto et al. 2006) and can cool the cortical surface to ~22°C within 30

Address for reprint requests and other correspondence: L. Krubitzer, Center for Neuroscience, 1544 Newton Ct., Davis, CA 95618 (e-mail: lakrubitzer@ucdavis.edu).

s. Although the portion of the device contacting the brain is small (4 × 4 mm and 2 mm thick), the entire device is larger. Long and Fee (2008) have developed a smaller Peltier cooling device to study neural mechanisms associated with birdsong. These devices are excellent for cooling very small brains; they have even designed an untethered device that can remove heat from subsurface (2-mm depth demonstrated) locations via insulated thermal probes (Aronov and Fee 2011). The main disadvantage is that these devices are designed to slow rhythmic behavior by cooling by 5–10°C rather than the 15–20°C required to abolish neural activity. These Peltier devices therefore may have a limited ability to transport sufficient heat passively across the larger distances required for mammals, especially in sulci where heat transfer across several centimeters of tissue may be required.

A cooling device currently in use in mammals is the cryoloop developed by Horel and colleagues (1992, 1984) and adapted by Lomber and Stein and their respective colleagues (Alvarado et al. 2007; Jiang and Stein 2003; Lomber 1999; Lomber et al. 1999). This device consists of stainless steel tubing through which chilled methanol is pumped and a thermocouple that monitors the cryoloop temperature. The size of this cryoloop ranges from about 4 to 10 mm in length, and in some laboratories (Lomber et al. 1999) up to 6 cryoloops have been chronically implanted in a single cat. The loops can be shaped to conform to the brain curvature and can be implanted within sulci, an important advantage. This device has been successfully utilized in studies of visual (Ponce et al. 2008; Rushmore et al. 2006), auditory (Lomber and Malhotra 2008; Lomber et al. 2007; Malhotra et al. 2008; Meredith et al. 2011; Payne and Lomber 1999), somatosensory (Alvarado et al. 2007; Jiang and Stein 2003), and posterior parietal cortex (Lomber and Payne 2001) to examine alterations in both neural response and behaviors when a target field is deactivated.

Despite its success, there are several limitations to the device. First, although it has been used successfully in acute preparations in smaller animals such as rats and guinea pigs (Antunes and Malmierca 2011; Coomber et al. 2011; Nakamoto et al. 2008, 2010), the size and weight of the entire device, including the connector head, may be too great to be used for chronic implantation in such animals. Second, because of the metal composition of the cryoloop, it is not magnetic resonance (MR) compatible. Third, cryoloops placed in the sulci cool both sulcal banks equally. Fourth, the standard device does not include a microthermocouple to record cortical temperature in chronic preparations (coolant tubing temperature is measured instead). Consequently, automated control of cooling based on thermal feedback from within the cortex has not been done. Thus, to date, there have been no cortical temperature data collected during task performance in chronic preparations. In acute experiments, temperature maps have been obtained via a hypodermic thermocouple after electrophysiological measurement was complete (Lomber et al. 1999). However, electrophysiological data and direct cortical temperature data are seldom collected simultaneously.

In this article we describe methods for fabrication and use of a lightweight, easily assembled, automated cooling device. This device can be implanted in one or more locations in the neocortex to study brain function and plasticity by reversibly disrupting or abolishing neural activity in a small volume of cortex. Our interest in cortical macrocircuitry and plasticity, and the need for a small, easy-to-use heat exchange device, were the motivations for the designs described. Compared with equipment currently used to study mammalian neocortex, our device, which we call a "cooling chip," along with connecting hardware, is smaller, lighter, more flexible and can be made to be MR compatible. It can be used to examine the brains of animals that range in size from rats to monkeys in both chronic and acute experimental preparations, and multiple cooling chips can be used in monkeys and other larger animals. Our cooling chip also contains a thermocouple in cortex providing feedback to a control circuit that maintains a desired in-cortex temperature in a restricted region. This represents a significant advance by expanding access to reversible deactivation techniques and extending them (especially for chronic implantation) to new animal models and cortical systems. We have conducted some pilot studies of chronic implantation of the device, but this report focuses on methods for acute preparations.

MATERIALS AND METHODS

The cooling device consists of the cooling chip itself and at least one thermocouple to record cortical temperature in or near layer 4. Electrodes for single- or multiunit electrophysiology may be lowered through ports in the chip to record neural activity in cooled cortex but are not necessary for cooling chip operation. While in use, the chip is connected to a peristaltic pump circulating chilled ethanol. The thermocouple implanted in the cortex provides temperature data that are used as feedback to control the coolant pump speed and to maintain the desired cortical temperature (Fig. 1). See Tables 1–3 for details on components and tools necessary to fabricate, implant, and operate cooling chips.

Design Specifications of the Cooling Chip

Materials. Our cooling chips are made of two materials. The first is the medical-grade silicone tubing through which the coolant, 100% ethanol, flows. The silicone is biocompatible and chemically compatible with ethanol (unlike polyurethane, it does not swell when exposed to ethanol). Tubing size and configuration vary according to the particular application. For use in rats and ferrets, we use tubing with a 0.51-mm inner diameter (ID), 0.94-mm outer diameter (OD), and a 0.22-mm wall thickness. We use slightly larger tubing (0.64-mm ID, 1.2-mm OD) for larger brained animals such as monkeys, which require greater heat transfer. The second material used for chip construction is polydimethylsiloxane (PDMS), a biocompatible polymer that is light and flexible. Created by mixing a siloxane base with a curing agent, uncured PDMS has a working time of about 2 h as a liquid with a viscosity similar to honey. Bubbles are removed by degassing in a vacuum chamber after mixing. Tubing is embedded in a thin layer of PDMS with the tubing that will contact the neural tissue slightly exposed. See Table 1 for a list of other materials.

Size, configuration, and fabrication. Cooling chips can be fabricated in various shapes and sizes. We use different designs for cooling of cortex on the gyral surface (Fig. 2, *A–D*) or within sulci (Fig. 2, *E–H*).

Coolant tubing in gyral chips forms a coil, often with two to four loops, embedded in a 1- to 3-mm layer of PDMS (Fig. 2, *A–D*). The edges of each coil-loop emerge <1 mm out of the PDMS on the side facing the cortex. The number and tightness of coils can be adjusted to create a footprint to match the area of interest. With four coils, this footprint covers a roughly circular 5-mm-diameter area. The chip also contains two to three prefabricated holes providing access to underlying cortex for electrodes and micro-

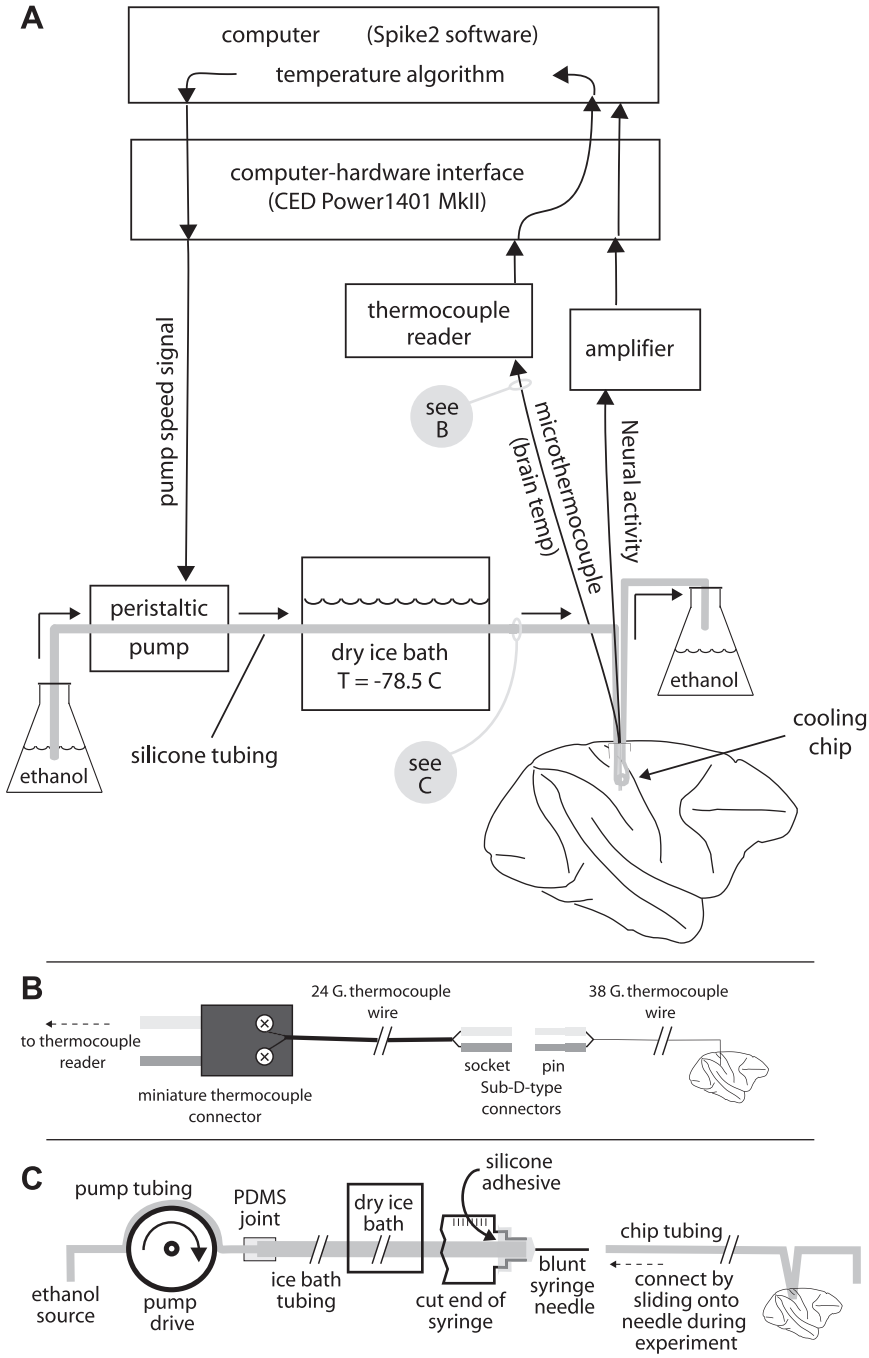

Fig. 1. Schematic illustration of equipment used during cooling. *A*: a peristaltic pump pushes ethanol through silicon tubing (thick gray line) that runs though a dry ice bath and then the cooling chip positioned on the cortex. A microthermocouple sends brain temperature data to a computer-hardware interface, a Power1401 mk II. An algorithm specified in Spike2 software uses this brain temperature as feedback to regulate pump speed, which is controlled by a voltage sent from the Power1401 to the pump. Neural activity from the electrode in the brain under the cooling device is amplified and recorded. *B*: connections between thermocouple reader and microthermocouple measuring brain temperature. *C*: tubing and tubing junctions. PDMS, polydimethylsiloxane.

thermocouples. The diameter of each port is large enough to accommodate both a recording electrode and a microthermocouple simultaneously.

Sulcal chips comprised coolant tubing that forms one or more hairpin turns in a single plane; single- or multiloop chips thus form the shape of the letters "U" or "W", respectively (Fig. 2, *E–H*). The thinness of this design (<2 mm thick, including PDMS) makes it appropriate for implantation within a sulcus. The PDMS insulates one side of the chip, allowing cooling of only one bank of a sulcus without affecting neural activity in the opposite bank (Figs. 2, *E* and *F*, and 8). The length of the footprint (5 mm in the chip shown in Fig. 2, *E–H*) can be adjusted to cool cortex in deeper sulci. Insulating PDMS could be included on parts of both sides, for example, to limit cooling to the fundus. Wider footprints can be achieved with additional loops and/or a larger bend radius.

SURFACE/GYRAL COOLING CHIP FABRICATION INSTRUCTIONS. Tubing coils are configured using a sheet of cellulose acetate as a template. Using a utility knife or scalpel with a pointed blade, create the acetate template by cutting two parallel slots and three holes in the configuration shown in Fig. 3*A*. Slot and hole width should equal the diameters of the tubing and metal rods, respectively. Thread the tubing and metal rods through the template as shown in Fig. 3*A*. Both tubing ends exit on the one side of the template. One to three metal rods (~1 cm long, 1 mm in diameter), which will be removed when the chip is complete, each provide a port for electrodes and microthermocouples to access cortex below the chip. Place the chip template at a >45° angle in a laboratory oven with the side of tubing ends facing down (so that the side that will contact the cortex faces up). Using a pipette, drip PDMS onto the acetate sheet above the coiled tubing and metal rods so that it

Table 1. *Materials for cooling chip fabrication and microthermocouple preparation*

Component or Tool/Part No.	Source	Quantity/Price, $	Per Chip
Gyral cooling chip			
Silicone tubing, biomedical (only 1 size per chip)			
0.51-mm ID/806400 (rats and small animals)	A-M Systems	20 ft/$18	25 cm/$0.72
0.64-mm ID/806700 (larger animals)	A-M Systems	20 ft/$23	25 cm/$0.92
PDMS, Sylgard 184 silicone encapsulant clear 0.5-kg kit			
184 SIL ELAST KIT 0.5KG	Dow Corning	0.5 kg/$60.48	20 g/$2.42
Acetate sheets, Grafix clear/55501-1303	Blick Art Supply	9 × 12 in., 25-pack/$7.27	5 × 5 cm/$0.01
Plastic transfer pipette/PTP-02	C&A Scientific	500/$17.50	1/$0.04
Stainless steel 304 hypodermic round tubing, 18 gauge			
B00137SLJ6 (metal rods to form ports in PDMS)	Small Parts	36 in./$3.53	3 × 1 cm (reusable)
Vacuum chamber jar with vacuum plate, Nalgene polycarbonate/polypropylene, 6 × 9 in./5305-0609	Amazon.com	$206.81	Reusable
Total price per chip			$3.19–3.39
Other tools: permanent marker, X-acto knife or scalpel, forceps, scissors, laboratory oven or incubator			
Sulcal cooling chip			
Silicone tubing, biomedical (only 1 size per chip)			
0.020-in. ID/806400 (for rats and small animals)	A-M Systems	20 ft/$18	25 cm/$0.72
0.025-in. ID/806700 (for larger animals)	A-M Systems	20 ft/$23	25 cm/$0.92
PDMS, Sylgard 184 silicone encapsulant clear 0.5-kg kit			
184 SIL ELAST KIT 0.5KG	Dow Corning	0.5 kg/$60.48	1 g/$0.12
Petri dishes, Fisherbrand Media-Miser, disposable			
60 × 15-mm (diam. × ht.)/08-757-13A	Fisher Scientific	500/$175.48	1/$0.35
Total price per chip			$1.19–1.39
Other tools: soldering iron, jumbo paper clip (wire for molding channel in petri dish), long-nose pliers, wire clippers, vacuum chamber (see above), drill			
Microthermocouples (2 per chip)			
Microthermocouple, 38AWG Bifilar 18.0-in. length/12117-1	R. T. D. Company	20/$728.00	1-2/$36.40–72.80
Thermocouple connector pins, sub-D type			
Constantan male pin/SMTC-CO-P	Omega Engineering	100/$63.00	1-2/$0.63–1.26
Copper male pin/SMTC-CU-P	Omega Engineering	100/$63.00	1-2/$0.63–1.26
Crimp tool, PremierMaster/IDE 28-512 (for connector pins)	Arcade Electronics	$141.96	Reusable
Total price per chip			$37.66–75.32

flows among the coils, producing a thin layer that covers all openings in the acetate (Fig. 3*B*). Incubate at 75°C for 1 h to completely cure the PDMS. (Higher temperatures will accelerate curing but will deform the acetate.) If the openings on the acetate sheet in between the coiled tubing are not sealed, repeat the previous step. Next, position on an oven rack with cortex side facing up. Using a pipette, add a second layer of PDMS up to a level <0.5 mm below the tops of the tubing coils (Fig. 3*C*). Incubate at 75°C for 2 h to completely cure. Next, remove the rods and gently peel back the acetate sheet, using water to help separate it from the PDMS. Use scissors to free the acetate, making cuts in the acetate sheet from the edge to the tubes. After the chip has been dried in the oven, replace the rods. Turn the chip upside down so that the cortex side faces down and secure tubing ends vertically above the chip (Fig. 3*D*). Add a third layer of PDMS ~1.5 mm thick. Incubate at 75°C for 20 min to partially cure PDMS. Slide fluorinated ethylene propylene (FEP; brand name "Teflon FEP") sheath (3.2-mm OD, 1.6-mm ID, ~35-mm length) over each silicone tubing end and press into soft PDMS, forming a circular groove (Fig. 3*E*). Introducing the FEP sheath after the PDMS is partially cured prevents PDMS from flowing up into the sheath and possibly constricting the silicone tubing. Incubate at 75°C for 2 h. The FEP sheath provides mechanical protection for the softer silicone coolant tubing and should be used if tubing might be constricted by dental acrylic, particularly during chronic implantation. Add a final layer of PDMS to cover just the remaining exposed tubing opposite the cortex side and incubate for 1 h (Fig. 3*F*). Repeat if necessary to fully protect and insulate tubing coils. After the final cure, remove the metal rods. PDMS surrounding the coils can be trimmed with scissors during surgery to fit the size of the craniotomy. Fabrication time is 2 h per chip plus 7 h of incubation time for PDMS curing.

SULCAL COOLING CHIP FABRICATION INSTRUCTIONS. The sulcal chip is easier to fabricate because it has only one or three simple hairpin turns; the process is different from that used to make coiled gyral chips. The materials necessary to make the sulcal chip are listed in Table 1. First, create a mold that will determine the shape of the hairpin turn and the amount that the tube protrudes from the PDMS. Bend a metal wire to the desired conformation of the coolant tubing loop. Wire diameter should be similar to or slightly smaller than that of the tubing; a "jumbo" paperclip (~47.5 mm long) is effective when working with tubing close to 1 mm in diameter. Position the wire such that the loop rests on the inside surface of a plastic petri dish as close to the dish wall as possible (Fig. 4*A*). While holding the wire loop in place, touch a soldering iron to the apex of the loop, heating the wire and melting a channel into the plastic. Next, drill two small holes through the base of the petri dish wall aligned with the ends of your loop mold and flush with the bottom of the petri dish. Thread silicone tubing through the holes, forming a loop that can be gently pressed into your mold (Fig. 4*B*). Next, pour PDMS into the dish to a depth of ~1.25 mm, and then incubate at 75°C for 3 h. Extract the chip by breaking the wall of the petri dish with wire clippers and slowly peeling the chip from the surface of the mold. Trim excess PDMS with scissors to the desired shape. Fabrication time is 45 min per chip plus 3 h of incubation. Multiple chips can be fabricated using the same dish.

Microthermocouple. The microthermocouple is made from insulated, flexible 38-gauge wires with a biocompatible polymer-coated tip (0.15 × 0.20-mm cross section). See Tables 1 and 2 for details of components and tools. Type-T thermocouples, which have an appro-

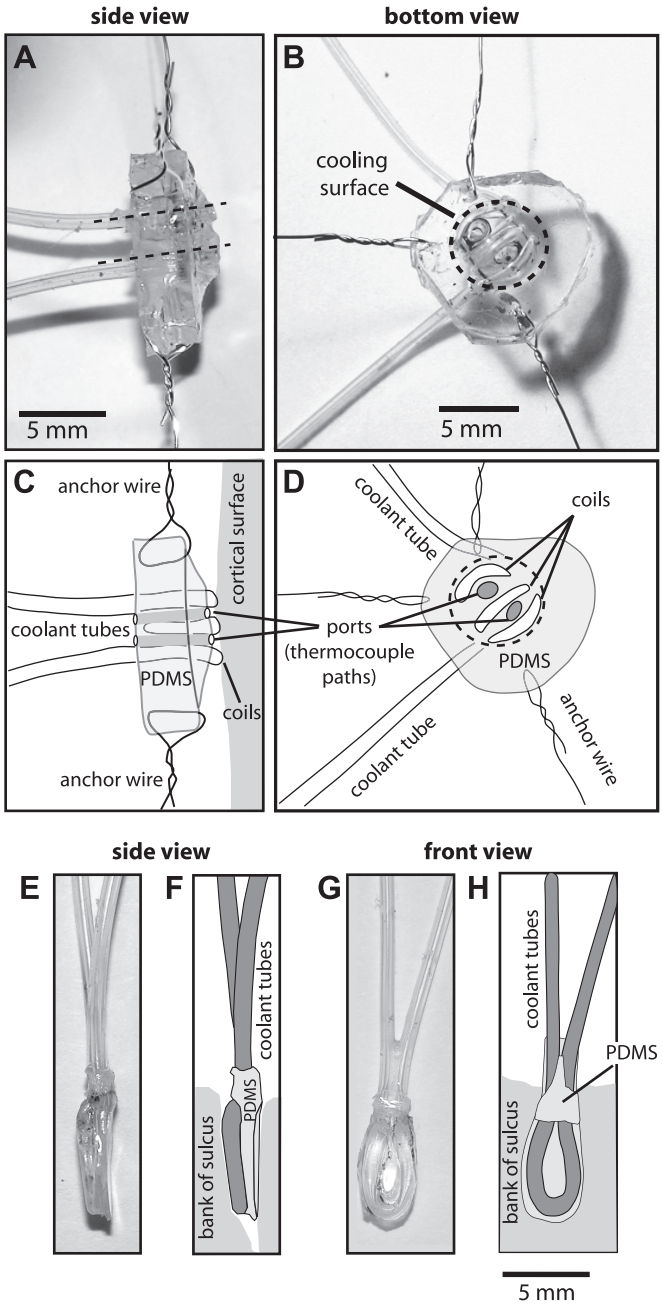

Fig. 2. Heat exchange devices ("cooling chips") for gyral and sulcal cooling. A coil-design gyral cooling chip is shown in a side (*A*) and bottom view (*B*). A drawing of the side (*C*) and bottom (*D*) of the device shows components labeled. The device consists of silicon tubing embedded in PDMS that can be trimmed to size during surgery. Preformed ports provide access to cortex below the cooling chip for microthermocouples and/or electrodes. A typical small coil design chip weighs about 0.4 g. Sulcal loop designs are shown from a side (*E*) and front view (*G*), and drawings of these sulcal chips are shown in *F* and *H*. The PDMS serves to insulate the opposite bank of the sulcus from cooling. The sulcal loop design (*E–H*) is smaller (0.16 g) than the coil design. For all of these cooling devices, microthermocouples and/or electrodes are positioned after the cooling chip is in place.

priate temperature range for biological applications, are composed of Cu and constantan (Cu-Ni alloy) wires. The point of measurement at the tip is the junction between these two metals; connector wires and junctions should be made of the same materials to avoid introducing additional measurement locations. Because of thermal conduction along the length of thermocouple leads, any such measurement in which leads cross a temperature gradient will be influenced by temperatures away from the theoretical measurement point (Tarnopolsky and Seginer 1999). This source of error can be reduced by using thinner thermocouple leads or alternative thermocouple types (such as type K) composed of metals with lower thermal conductivity.

Leads are fitted with male Cu and constantan crimped sub-D-type pins of the kind found in many older computer connectors (Fig. 1*B*). Such pins (Fig. 1*B*, *right*) are substantially smaller than miniplugs (Fig. 1*B*, *left*; depicted to scale relative to sub-D pins), a particular advantage for chronic implantations. A previous study in which cooling devices were chronically implanted in cats included a female miniplug in the implant, which is the same size or slightly larger than the housing of the male miniplug depicted in Fig. 1*B* (Lomber et al. 1999). Individual female sub-D sockets insulated with heat-shrink tubing (for mechanical support and to prevent shorting) can be quickly and reliably connected during testing. Female sockets are connected to type-T miniplugs via 24-gauge thermocouple wire. Cortical temperature from one or more sites and rectal temperature are measured with a four-channel thermocouple meter and recorded via the computer-hardware interface. Monitoring core body temperature is particularly important for small animals in which cooling the cortex triggers an automatic homeostatic response to raise body temperature to overcome the heat loss in the cortex.

Peristaltic pump and dry ice bath. During cooling, tubing from the cooling chip is connected to a larger circuit comprising a peristaltic pump, which pushes ethanol coolant through a length of tubing running through an ethanol-dry ice bath (−78.5°C) and then through cooling chip tubing (Fig. 1*C*). See Table 2 for components used during operation of the cooling chip. It is essential that the ethanol remain 100% dehydrated, because water ice could block coolant flow. The length of tubing between the dry ice bath and the chip should be minimized (<50 cm) to reduce heat absorption through the thin tubing walls.

Automated control of coolant pump with feedback from thermocouple in cortex. Cortical temperature data are recorded and provide input to Spike2 software as feedback to control coolant pump drive speed to achieve and maintain a target temperature (Fig. 1). Analog voltage (0–10 V) sent from the computer-hardware interface to the pump specifies speed (0–100 RPM) and therefore coolant flow rate (equivalent to 0–7.5 ml/min of coolant with 1.30-mm-ID tubing running through the pump head rollers).

A typical cooling session to reduce cortex temperature to 19°C (see Fig. 6*B*) begins with coolant flow of 4.5–7.5 ml/min (60–100% of maximum pump speed), which slows as the temperature approaches 19°C and eventually stabilizes at 2.25–4.13 ml/min (30–55% maximum). The flow rate is automatically adjusted for a predetermined temperature drop while minimizing the probability of overshooting the target temperature, which could potentially damage superficial layers of cortex. Because each chip-cortex interface has different heat exchange properties, rapid feedback and a robust flow rate control algorithm are necessary to ensure safe and effective cooling. We have developed a flow rate control algorithm encoded in a Spike2 script that produces rapid cooling and establishes a stable target temperature. We employ a custom proportional-integrative-derivative (PID) control algorithm to regulate pump speed. A PID algorithm combines three weighted comparisons. *1*) The proportional term is simply the instantaneous error, e_t at present time t, that is, the current temperature (T_t) minus the target temperature (T_{target}). Larger values result in higher pump speeds. *2*) The integrative term examines past performance by integrating e_t within a specified time window. The use of this term can reduce steady-state error if the weighting of the proportional term is not appropriate. For example, if $T_{target} = 25$°C but T_t is a steady 27°C, the proportional term will be relatively small but the consistent positive error will be evident in the integrative term. *3*) The derivative term, or rate of change in e, effectively looks at future performance and can be used to prevent overshoot caused by large integrative terms. Overweighting of the derivative term can lead to oscillations in temperature. Our PID algorithm achieves a rapid drop in brain temperature (decrease

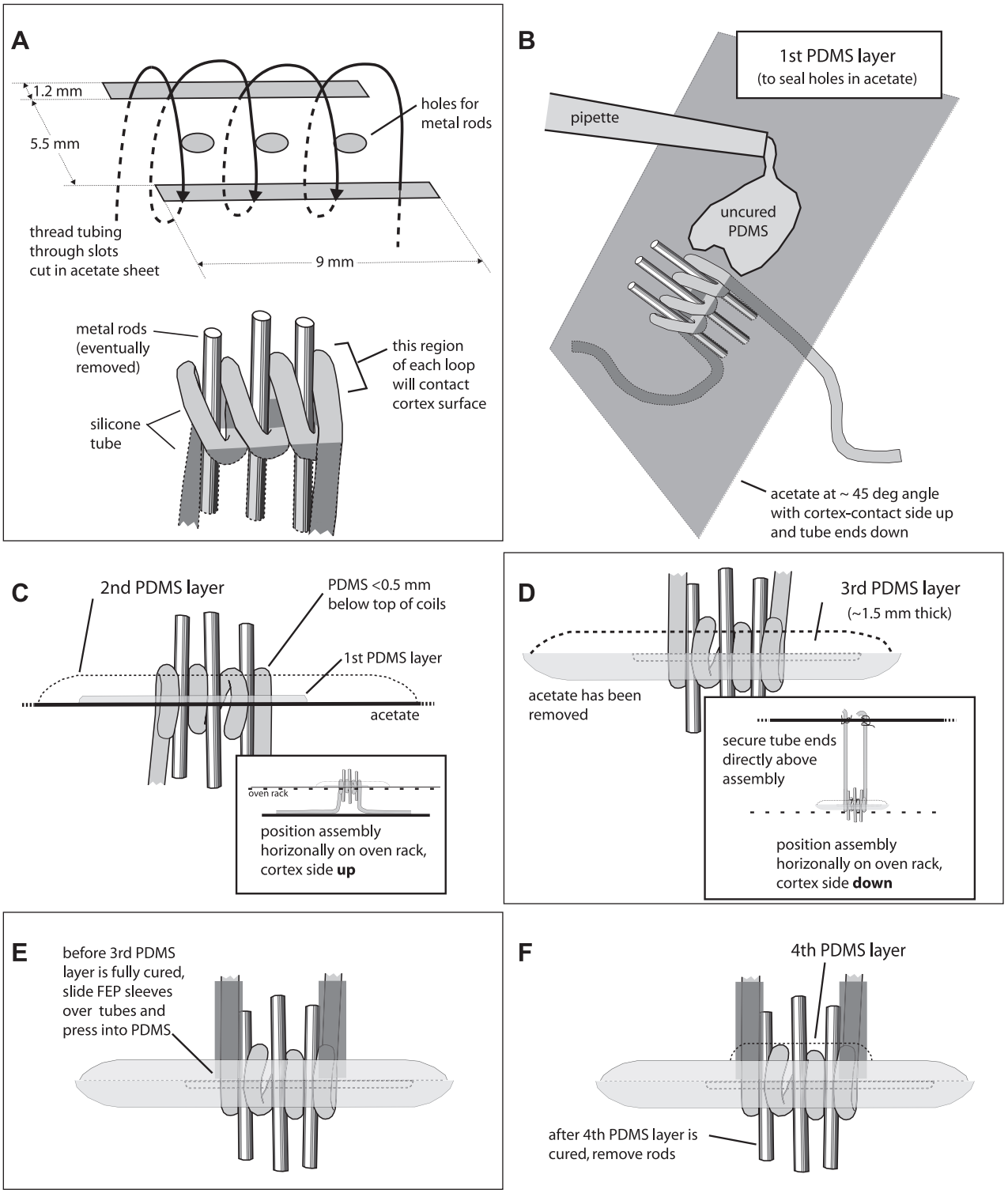

Fig. 3. Instructions for fabrication of cooling devices for implantation on gyral surface. *A*: create a temporary framework by cutting holes in an acetate sheet (*top*) through which silicone tubing is threaded to form a coil or helix with both ends exiting opposite to the side that will contact the cortex. Insert metal rods (*bottom*) through the acetate to form a template for holes within the coiled region for insertion of electrodes and thermocouples. *B*: position acetate at an angle with the cortex side up and drip only enough uncured PDMS to close remaining gaps in acetate around the tubing and rods. *C*: after the PDMS has cured, position the cooling chip with the side that will contact the cortex facing up (*inset*) on oven rack, add second PDMS layer, and cure. *D*: position the chip with cortex side down and secure tube ends above to create desired tube exit angle (*inset*). Add third PDMS layer. *E*: before third PDMS layer is fully cured, slide fluorinated ethylene propylene (FEP) sleeves (dark gray) down tubing and press into PDMS. *F*: add fourth PDMS layer to protect and insulate top of coils. After curing, remove rods, providing paths for microthermocouples, guide tubes, and/or electrodes.

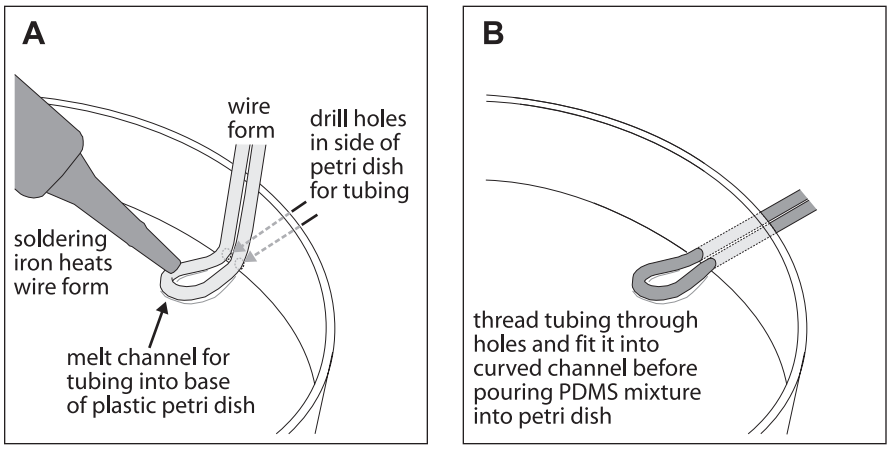

Fig. 4. Instructions for fabrication of cooling devices for implantation in sulcus. Shape a wire (same diameter as tubing) with pliers, and then place it on the bottom of a plastic petri dish and heat to melt a channel (*A*). Drill holes of the same diameter in base of petri dish side. Thread tubing through holes and fit into channel in bottom of dish (*B*). Not shown: pour liquid PDMS mixture into dish to desired depth and allow to cure; break dish to extract cooling device; and trim excess PDMS.

of 17.5°C in 46 s in an awake monkey) with transient overshoot of no more than 1–2°C. Stability is excellent for at least 1 h, with error usually less than ±0.3°C after recovery from any overshoot (see Fig. 6*B*).

Algorithm. This algorithm is designed to achieve three goals: *1*) quickly cool cortex temperature; *2*) avoid overshooting T_{target} during the initial cooling; and *3*) maintain the pump speed that resulted in the T_{target}, adjusting the speed if conditions change. Our algorithm functions through three separate states.

State 1: If $e_t > 1$°C, run pump at maximum speed $V = V_{max}$. *State 1* is the initial state for every cooling run. At this point, brain temperature is higher than T_{target}. To achieve the target temperature quickly, the pump is run at a specified maximum speed until the brain

Table 2. *Materials for operation of cooling chip*

Component or Tool/Part No.	Source	Quantity/Price, $	Usage
Computer-hardware interface			
Power1401 mk II with Spike2 software	Cambridge Electronic Design	$9,475	1
Coolant circuit			
Pump			1/Active chip
Masterflex L/S computer-compatible digital drive/EW-07551-10	Cole-Parmer	$2,095	
Ismatec minicartridge pump head/EW-07623-10	Cole-Parmer	$545	
Adaptor cable (connects pump to computer-hardware interface) male DB25 to 2 BNC connectors/custom order	Cabledepot.com	$35	1/Active chip
On DB 25, pins 1 and 3 (signal, ground) are speed control input to pump (0–10 V, 0–100 RPM); pins 14 and 5 (signal, ground) are speed signal output from pump (0–10 V)			
Tubing set (runs from ethanol source to cooling chip tubing)			1/Active chip
Pump tubing			1/Tubing set
Ismatec three-stop color-coded autoanalysis tubing/HV-95603-32	Cole-Parmer	6/$61	Replace after 4 mo
Runs from ethanol source, through pump head rollers, and connects to dry ice bath tubing			
Dry ice bath tubing			
Biomedical silicone, 0.762-mm ID/807000	A-M Systems	20 ft/$23	4 ft/Tubing set
Connects to pump tubing via PDMS seal, runs through ice bath for ~60 cm, connects to cut end of 1-ml plastic syringe with silicon adhesive. Syringe needle fits on syringe tip.			
Syringe needle, stainless steel blunt needle with Luer polypropylene hub, 21 gauge × 1/2-in. length	Amazon.com	25/$7.49	1/Tubing set
Connects to cut syringe on tubing. Inserted into cooling chip tubing during experiments. Fits 0.508- and 0.635-mm ID chip tubing.			
Other components: PDMS (seal connections between pump and ice box tubing), silicone adhesive (glue ice bath tubing to syringe), 1-ml plastic syringe, polystyrene cooler (dry ice bath, lined with plastic sheeting) filled with 100% ethanol and chunks of dry ice, sand paper (to roughen outer surface of syringe needle), BNC cable			
Temperature measurement			
Thermocouple Meter/TC-2000	Sable Systems	$1,800	1 meter/4 Thermocouples
Thermocouple connector sockets, sub-D type (connect to implanted thermocouple pins)			1 pair/Thermocouple
Constantan female socket/SMTC-CO-S	Omega Engineering	100/$63	
Copper female socket/SMTC-CU-S	Omega Engineering	100/$63	
Thermocouple wire, T-type, Duplex insulated, 24-gauge TT-T-24S-50 (connects sockets to mini connectors)	Omega Engineering	50 ft/$40	2 ft/Thermocouple
Miniature thermocouple connectors, male/SMPW-T-M (connect to thermocouple meter)	Omega Engineering	1/$1.75	1/Implanted chip
Other components: BNC cables (thermocouple meter to computer-hardware interface), 5-mm-diam. heat-shrink tubing (for female thermocouple sockets)			

Table 3. *Materials for surgical implantation (beyond standard tools for craniotomy)*

Component or Tool/Part No.	Source	Quantity/Price, $	Per Surgery
Sheet metal screw, stainless steel (skull screw for acute preps)			
Phillips drive no. 4, oval head (ferrets)	Ace Hardware	1/$0.12	0–4
Phillips drive no. 2, flat head (rats)	Ace Hardware	1/$0.12	2–4
GLUture topical tissue adhesive/32046-01	Abbott Laboratories	1.5 ml/$19.49	Varies
Tungsten carbide needle for microdissection, 1-μm tip diameter			
Tungsten needles, rod diam. 0.25 mm/10130-10	Fine Science Tools	10/$86.50	1–2
Nickel-plated pin holder, 17 cm/26018-17	Fine Science Tools	$19.75	Reusable

temperature is <1°C above T_{target}, at which point the algorithm switches into the second state.

State 2: If $e_t \leq 1$°C (and does not meet the criteria for *state 3*), then the pump speed V is as follows:

$$V = R + K_x \ln \frac{T_t + K_d \frac{d}{dx} e(t)}{T_{target}} \quad (1)$$

(If $V > V_{max}$, run at V_{max}. If $V < 0$, run at 0.) In *Eq. 1*, K_x is a general tuning parameter, K_d is a tuning parameter for the derivative term, and R is a recursive term, including an integration of error over the previous 5 s:

$$R_n = R_{n-1} + K_i \int_{-5}^{0} e(\tau) d\tau \quad (2)$$

where K_i is the integral tuning parameter. At *time 0*, R is seeded with a user-defined pump speed (based on previous sessions) that yields T_{target}. The closer this term is to the pump speed that achieves T_{target}, the faster cortical temperature will stabilize.

State 2 dynamically adjusts pump speed, where V represents the pump speed in RPM. *State 2* operates on the basis of a modified PID formula, which allows for continued cooling without the risk of a significant overshoot while T_t approaches T_{target}. The second term in the *state 2* equation contains the derivative of error, calculated as the mean of $e_{0\ to\ -1}$ minus $e_{-1\ to\ -2}$. Once the brain temperature is within ± 0.1°C of T_{target} and has stabilized, the algorithm switches into *state 3*.

$$\text{If} \quad K_i \int_{-10}^{-5} e(\tau) d\tau - 0.01 < K_i \int_{-5}^{0} e(\tau) d\tau < K_i \int_{-10}^{-5} e(\tau) d\tau + 0.01 \quad (3)$$

$$\text{and} \quad \left| K_i \int_{-5}^{0} e(\tau) d\tau \right| < 0.1, \quad (4)$$

then maintain current pump speed (V).

State 3 maintains the pump speed that resulted in a stable achievement of target temperature. Stability is determined by comparing error integrated over two time periods: -5 to 0 s and -10 to -5 s. If in these periods the error changes by <0.01°C and the error in the more recent period is <0.1°C, *state 3* continues and V will not change. Should these conditions change, the algorithm will switch back into one of the two preceding states, depending on how great a temperature difference is produced. This allows the algorithm to quickly respond to any physiological changes that might occur throughout the course of an experiment and find a new pump speed that will produce the desired target temperature.

Microelectrode. Microelectrodes are not necessary for regulation of cooling, but we collected data on neural activity to provide additional information on deactivation dynamics. Standard epoxy-coated tungsten electrodes (5 MΩ, tip exposures <30 μm; A-M Systems, Sequim, WA) were lowered using a micromanipulator (Kopf Instruments, Tujunga, CA) to record extracellular activity from neural clusters and single neurons. Neural activity was amplified and filtered (model 1800 amplifier; A-M Systems), captured and quantified (CED Power1401 mk II hardware with Spike2 software), monitored through a loudspeaker, and visualized on a computer monitor.

Surgical Procedures

We tested and refined surgical procedures and devices on four rats (*Rattus norvegicus*, 225–425 g), seven ferrets (*Mustela putorius*, 650–900 g), and two monkeys (*Macaca mulatta*, 14.1–14.6 kg). Cooling devices were also implanted chronically in one additional rat (600 g), ferret (825 g), and monkey (13.0 kg). All acute experiments were completed under aseptic conditions, and all chronic surgeries were completed under sterile conditions. All animal protocols were approved by the University of California, Davis Institution Animal Care and Use Committee and conform to National Institutes of Health guidelines.

The cooling chips were implanted in different ways depending on the size of the brain, location within the brain, and whether the experiment was acute or chronic. Here we only describe the placement for acute experiments. See Table 3 for details on components used during implantation.

Rats. Rats were anesthetized, and core body temperature, heart rate, and respiration rate were continuously monitored. Once the animal was anesthetized, the skin was cut, the temporal muscle was retracted, and holes for three skull screws were placed around the planned craniotomy. The bone over the area of interest was removed, and skull screws were placed (Fig. 5). In four of five rat cases, the dura was cut and the cortex was exposed, whereas in one case, the dura was left in

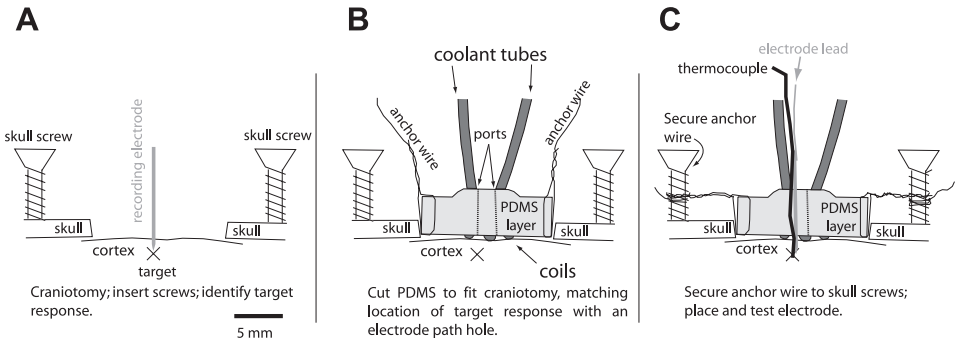

Fig. 5. Surgical procedures for acute use of the gyral cooling device are illustrated (*A–C*). See text for details.

place and recordings were made by lowering electrodes through the dura. A digital image of the brain was taken and printed so that the location of the electrodes, thermocouples, and the cooling chip could be documented relative to vascular patterns. Electrophysiological recordings in somatosensory cortex were used prior to chip placement to determine an optimal location in which to test the device (see below).

Once the location for placement of the chip was ascertained, the cooling chip was cut out of the PDMS sheet so that only a small margin of PDMS surrounded the chip (Fig. 5*B*). Three to four 0.25-mm-diameter anchor wires were threaded through the PDMS margin of the chip. The chip was centered over the area of interest, and the anchor wires were twisted around the screws surrounding the craniotomy (Fig. 5*C*). Next, the electrode and thermocouple were lowered through cooling chip ports to monitor neural activity and temperature under the chip, or were lowed into cortex at locations up to 2 mm away from the chip. The effects of cortical cooling are described in RESULTS.

Ferrets and monkeys. Ferrets and monkeys were tracheotomized and intubated, respectively. Monkeys were cannulated and given a continuous infusion of 2.5% dextrose in lactated Ringer (6 $ml \cdot kg^{-1} \cdot h^{-1}$ iv), alternated with lactated Ringer alone. Ferrets were kept hydrated with regular subcutaneous injections of lactated Ringer (up to 10 $ml \cdot kg^{-1} \cdot h^{-1}$). Inhalation anesthesia was administered (1–2% isoflurane). Temperature, heart rate, blood oxygenation levels (in monkeys only), and fluid intake and output were monitored (Padberg et al. 2010). We used surgical and implantation procedures similar to those described above for some of the ferrets. In other ferrets and in both monkeys, we used an alternative method that did not include skull screws or anchor wires. Because the slope of the brain in the areas of interest in both ferrets and monkeys was less steep than that in rats, positioning the cooling chip on the cortical surface was relatively easy.

Once the region to be cooled in somatosensory cortex had been chosen, the PDMS chip margin was cut to fit the edges of the craniotomy and the chip was placed over the area of interest. The edges of the PDMS were secured to the dura or skull with GLUture topical tissue adhesive (see Table 3). This reliably maintained chip position for the remainder of acute experiments (>24 h in some cases), but the chip could be removed and repositioned if necessary.

For the placement of sulcal cooling chips, the pia spanning the sulcus was cut with Vannas scissors and a tungsten microdissection needle or fine-gauge syringe needle, with special care taken to avoid large blood vessels. Cotton swabs and ophthalmic spears were used to open the sulcus. After placement, chips were secured to the surrounding dura using surgical glue and held in place with thin sheets of PDMS positioned on the gyral surface around the chip's periphery.

Electrophysiological recordings for implantation placement and testing of cooling efficacy. Before placement of the cooling chips, electrophysiological recordings (electrodes and recording apparatus are described above) were used to identify the boundaries of the field of interest. A number of closely spaced recording sites were tested and marked on an enlarged digital image of the brain. At each site, receptive field and stimulus preference were obtained. For all animals, we placed our cooling chips in somatosensory cortex. In rats and ferrets the cooling chip was placed over the vibrissae/face representations of S1, and in monkeys the cooling chip was placed over the hand representation of areas 1 and 2.

Somatosensory stimulation of cutaneous receptors consisted of lightly touching or brushing the skin or deflecting hairs. Stimulation of deep receptors included light pressure, lightly tapping the skin, or manipulating joints. Such stimuli have proven effective for determining the extent of the cortex devoted to a particular sensory system and for determining the boundaries of cortical fields within a given sensory system in previous mapping studies in primates (Krubitzer et al. 2004; Padberg et al. 2005, 2007; Seelke et al. 2011).

Once the location of chip placement was determined, a controlled somatosensory stimulator was used to quantify neural responses. The stimulator consisted of a solenoid valve (activated by the software via a relay) that started and stopped a stream of pressurized air. This air stream passed through an adjustable nozzle (Loc-Line; Lockwood Products, Lake Oswego, OR) and could be precisely aimed to stimulate a somatosensory receptive field. Spike2 software controlled the timing and duration of air puffs through digital voltage output from the Power1401 hardware to the solenoid relay. After localization and quantification of receptive fields, the chip was implanted (see above) and the electrodes were secured. The sensory-driven responses of neurons at sites below and around the chip at different cortical depths were systematically studied throughout the cooling process.

RESULTS

Here we describe several aspects of the performance of the cooling chip. First, we describe the heat exchange capabilities of the cooling chip at the tissue interface and our ability to control cortical temperature. Second, we demonstrate the spatial extent of cortical temperature change. Third, we show the relationship between cortical cooling and both spontaneous and sensory-driven neuronal activity. Fourth, we examine the longevity and functional durability of these chips in chronic experiments in rats and ferrets. Finally, we describe preliminary data on MR compatibility of the cooling device.

Coolant Flow Rate and Control of Tissue Temperature

We examined the effect of coolant flow rate on the rate of cooling and equilibrium cortical temperature to define the relationship between the two. For example, in superficial layers of ferret somatosensory cortex, at a constant coolant flow rate of 3.4 ml/min through a gyral design chip, temperature at a depth of 800 μm declined from 37 to 15°C within 60 s (Fig. 6*A*). At a slower flow rate (2.2 ml/min), the same temperature reduction was achieved in 90 s. When the flow rate was too slow (1.0 ml/min), target temperature could not be reached. Heat exchange is also affected by other factors such as tubing diameter and wall thickness as well as area of tubing contacting the cortical surface, so in another preparation similar flow rates could lead to different cortical temperatures, although higher flow rates would still decrease the temperature more rapidly.

By providing cortical temperature feedback to the control algorithm that continually alters pump speed (see MATERIALS AND METHODS), we could specify a target temperature that could be achieved quickly and accurately (Fig. 7) and be maintained for at least 1 h (Fig. 6*B*). This also allowed our equipment to respond to any physiological changes that may have altered heat exchange at the chip/brain interface. Figure 7 shows active cooling and passive warming in 5°C steps and active cooling in 1°C steps. "Passive" warming was not completely passive: it was regulated to avoid overshoot by increasing coolant flow rate to slow warming as temperature approached the target. The gray boxes in Figs. 6*B* and 7 show the investigator-specified target temperature ±0.3°C. After an initial temperature overshoot of <0.5°C, temperature was maintained within ±0.3°C.

Spatial Extent of Cooling

The effect of increases in coolant temperature as it moved through successive coils of a gyral cooling chip in contact with the brain was found to be relatively small (<2°C) as measured at two locations under the cooling chip (compare solid and dashed traces in Fig. 6*A*).

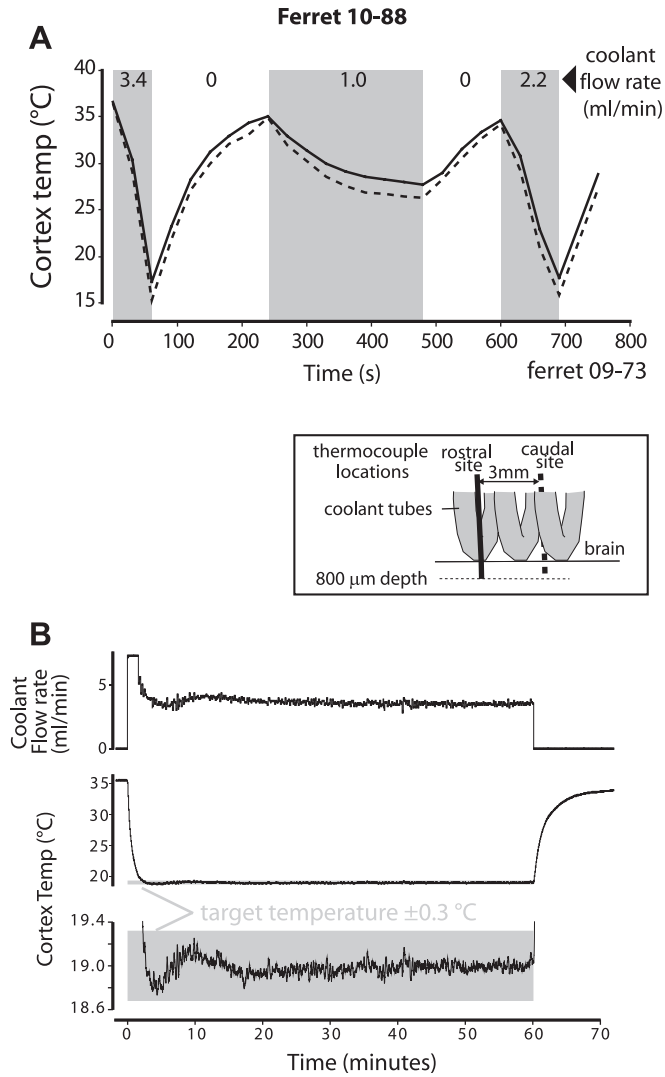

Fig. 6. Parameters affecting cortical cooling. *A*: cortical temperature was measured at different constant pump speeds in *ferret 09-73*. Measurements were made simultaneously at caudal (dashed lines) and rostral (solid lines) locations under a gyral design cooling chip (see *inset*, *A*). The similarities of the dashed and solid traces (corresponding to the caudal and rostral recording sites) indicate that the cooling properties across the chip were fairly uniform. Faster coolant flow rates generated faster cortical cooling. Shaded areas indicate time periods when the pump is on; numbers at *top* indicate the pump speed in ml/min. *B*: use of feedback to maintain a stable cortical temperature. Unlike in *A*, where the pump was fixed at various constant speeds, here an algorithm controlling coolant pump speed (*top* plot, flow rate) with feedback from cortex temperature regulated the cooling of cortex to 19°C and maintained that temperature to within 0.3°C for 60 min (*ferret 10-88*). *Bottom* plots show temperature data at 2 different *y*-scales. Gray boxes indicate experimenter-specified target temperatures (±0.3°C). All cooling chips used to generate data for this figure were the gyral design constructed from tubing with 0.51-mm ID.

Sulcal cooling chips are insulated such that the two sulcal banks are cooled asymmetrically (see MATERIALS AND METHODS). We tested the effectiveness of this insulation during cooling by measuring in-cortex temperature in each bank. Cortex adjacent to the insulated side of the cooling chip was slightly cooled, but substantially less than the opposite bank (Fig. 8). Therefore, cooling can be regulated such that one bank is deactivated while the other remains warm enough to maintain neural activity.

The temperature gradient below and lateral to the cooling chip defines the effective virtual lesion. We measured the spatial extent of cooling in *monkey 10-159* while achieving a target temperature of 22.5°C at a depth of 1,000 μm directly under the cooling device (blue circle in Fig. 9). Temperature was also measured on separate cooling sequences at various depths and lateral distances from the cooling device (other circles, color-coded by temperature). A uniform flow rate of 6.75 ml/min was used on all sequences. Temperature data were recorded when the target location 1,000 μm under the cooling chip reached 22.5°C. Not surprisingly, locations in cortex closest to the cooling chip were coldest, and as cortical depth increased, so did temperature. The gradient was steepest closer to the cooling chip (5.6°C/mm). Cortex only 500 μm lateral to the cooling device was much warmer (29.8–32.5°C), and the lateral thermal gradient was shallower (0.8°C/mm at 1,000 μm).

A mathematical model was developed to predict the effective volume of a cooled region of cortex as a function of cooling device geometry, flow rate, and cortical thickness. The strategy was to model the heat transfer properties of the cooling chip on cortices with varying thickness and vasculature. As a first approximation, we modeled heat transfer in the brain using the well-known Pennes bioheat equation:

$$\rho c \frac{\partial T}{\partial t} = k\nabla^2 T + \rho_b c_b \omega (T - T_b) + q''' \qquad (5)$$

where ρ, c, and k respectively denote the density, specific heat capacity, and thermal conductivity of brain tissue, ρ_b and c_b respectively denote the density and specific heat capacity of

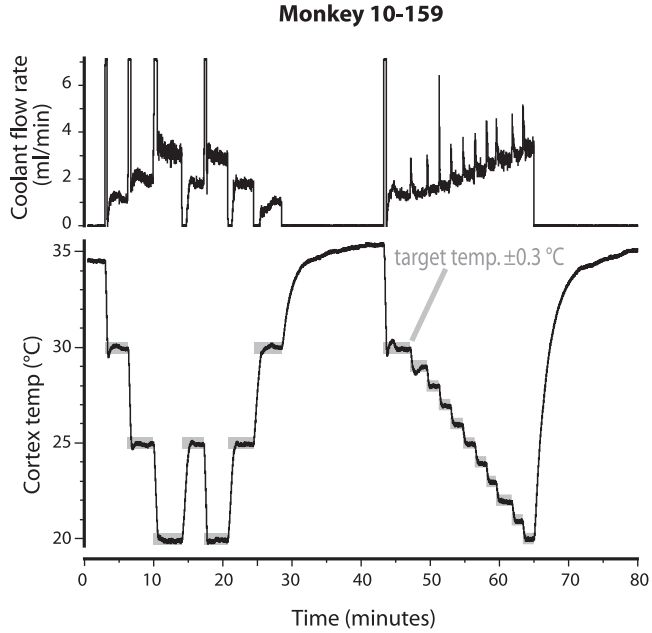

Fig. 7. Automated feedback control of brain temperature (*bottom* trace) by regulation of coolant flow rate (*top* trace) in anesthetized *monkey 10-159*. Temperature was recorded from a microthermocouple in cortex 600 μm below a cooling chip located on the pial surface of area 2. Gray boxes indicate experimenter-specified target temperatures (±0.3°C). Target temperature was achieved in <60 s. Overshoot was <0.5°C, and postovershoot was well within ±0.3°C. Resting temperature (~35°C) was several degrees lower than normal because brain was exposed to the air. Automated feedback control performance was similar in awake monkeys.

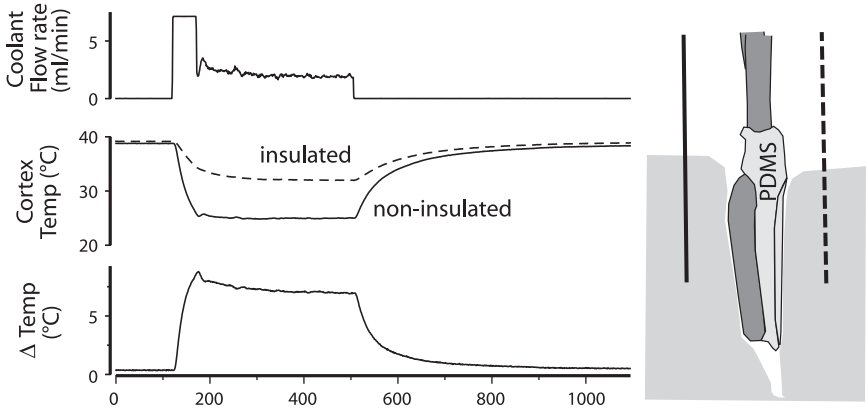

Fig. 8. Differential cooling of sulcal banks. Temperature was measured in both banks of the intraparietal sulcus in *monkey 10-172* while a sulcal cooling chip was activated. In the schematic diagram at *right*, the thermocouple on the bank exposed directly to the coolant tubing (non-insulated) is shown as a solid line. The thermocouple on the bank insulated by a layer of PDMS is shown as a dashed line. *Top* trace shows coolant flow rate. *Middle* traces show temperature in the non-insulated (solid line) and insulated (dashed line) banks of cortex. *Bottom* trace is the difference (Δ) in temperature between the banks.

blood, ω is the volume fraction of the brain that is occupied by blood vessels, and T_b is the temperature of blood (typically 36.65°C). The second term on the right is known as the blood perfusion term, which incorporates the thermal effects of blood flow within the brain. The third term, q''', represents metabolic energy.

We approximate the primate brain as a hemisphere with a radius of 50 mm. The domain boundaries are assumed to be insulated (zero heat flux) everywhere except the points of entry and exit of the ethanol. The point at which ethanol enters is modeled as a constant temperature boundary condition with temperature T_{in}, whereas the point at which ethanol exits is modeled as a time-varying temperature, T_{out}. It is thus critical for the success of the model to accurately measure T_{in} and record T_{out} for the duration of the experiment. Because the model will include the entire cooling chip, whose geometry can be quite complex, it will be solved using a three-dimensional finite element method. The model will be refined by adding information from data gained from cooling chips around large blood vessels. Our strategy is to utilize this model as a basis for developing scaling laws that will facilitate design changes between the smaller chips used in rodents and the larger ones that accommodate the larger size and blood vessel density of monkey brains.

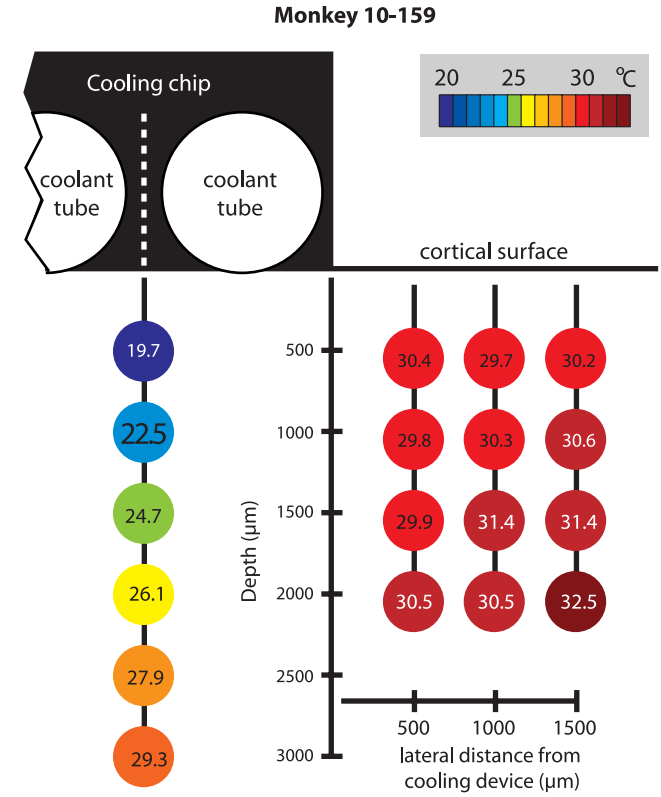

Fig. 9. Spatial extent of cooling in monkey *10-159*. Microthermocouples were lowered into the brain both through a port in the cooling chip (dashed white line between coolant tubes) and at 3 locations lateral to the chip. For a target temperature of 22.5°C at a depth of 1,000 μm under the cooling chip, temperature was also measured at various depths and lateral distances from the cooling device. Each location is color-coded by temperature (see key, *top right*). Under these conditions, cortex lateral to the chip was substantially warmer than cortex directly under the chip.

Neural Activity

We examined the effects of cortical cooling on spontaneous and sensory-driven neuronal activity. In all species, sensory-driven activity was abolished at 20°C or below (Figs. 10 and 11). Spontaneous activity was often disrupted, as well. We ran several consecutive cycles of active cooling followed by passive rewarming (Figs. 10 and 11; cooling runs shown in Figs. 10 and 11 were performed with manual pump control before feedback-driven computer control such as that shown in Figs. 6 and 7 was implemented). Figure 10 shows data from *ferret 09-31* in which neurons were driven periodically by manual stimulation of the somatosensory receptive field on the face. Stimulus timing was approximated with a coincident keystroke for each touch to the ferret's face. In contrast, a computer-controlled air puff was used to stimulate neurons' receptive field in *monkey 10-21*, so timing was precise. In both animals, neurons and temperature were recorded in cortex directly below a cooling chip. Responses to individual stimulus events can be seen in the expanded temporal views (gray regions, Figs. 10*A* and 11*A*, *bottom*) and in the spike rasters (Figs. 10*B* and 11*B*). Traces to the *right* of the rasters show the mean spike rate (black) and temperature (gray) during cooling. Solid black traces are driven activity, and dashed traces are spontaneous activity. In both the ferret and monkey, neural responses declined or vanished during cooling and recovered after rewarming. Spontaneous activity also decreased during cooling, although in some other cases, spontaneous activity increased during cooling (data not shown). Driven neural activity and cortical temperature were tightly coupled, although our data show some delay. Post mortem examination revealed no visible tissue damage below the cooling chip.

Chronic Implantation

The third stage of experimentation was to observe the functionality and biocompatibility of cooling chips and

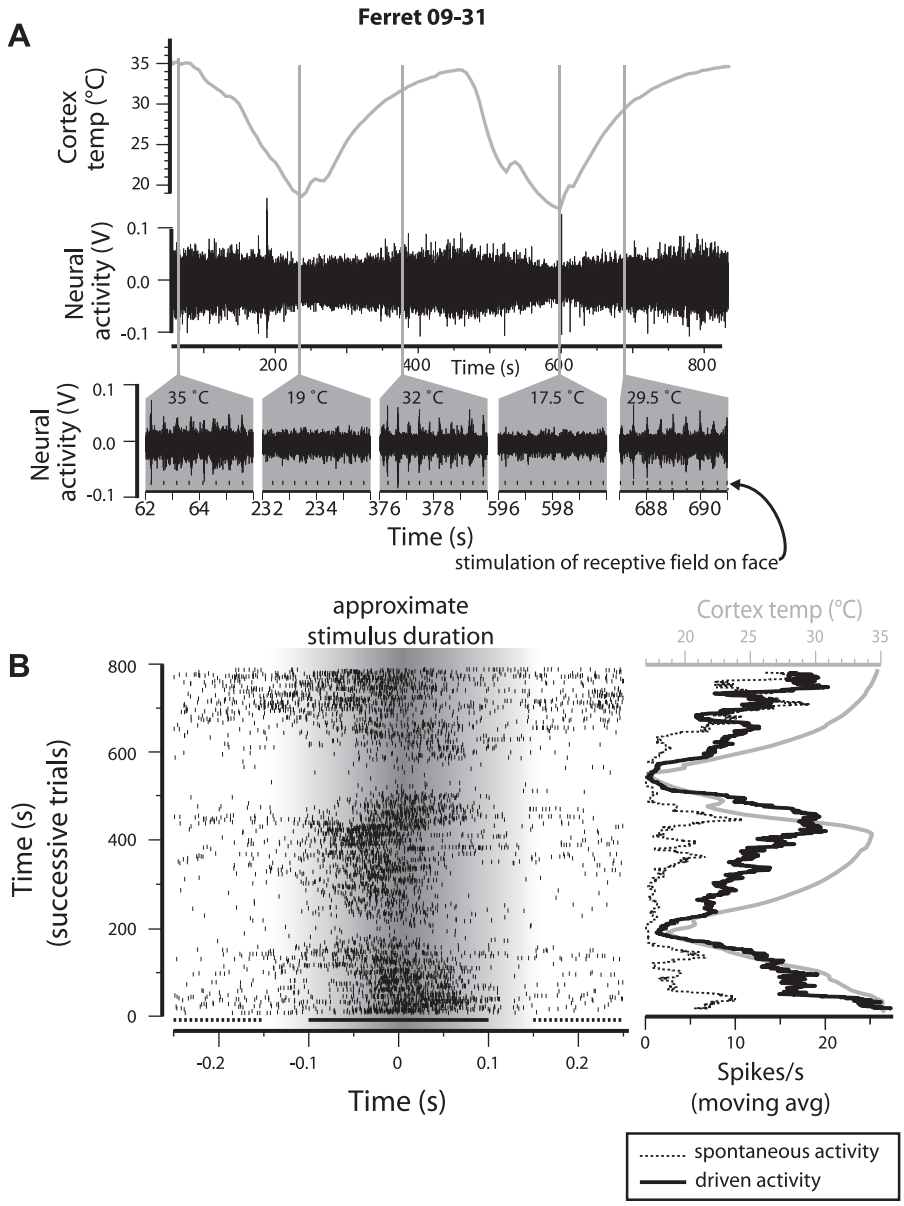

Fig. 10. Spontaneous and sensory-driven neural activity in area 3b of *ferret 09-31* during cooling. The receptive field for neurons below the chip (in cortical layer 4) was determined and systematically stimulated while the cortex was locally cooled, and neural activity and local cortical temperature were monitored simultaneously. *A*: temperature (gray trace) and cortical activity (black trace) during 2 consecutive cooling sessions. Coolant flow rate was controlled manually. *Bottom* panels in *A* show expanded views of neural activity at different time periods over the 2 cooling sessions. Tick marks below these traces indicate the timing of tactile stimulation. The receptive field on the face of the ferret was manually stimulated with the use of a paintbrush at ~2 Hz. *B*: spike rasters aligned to approximate onset of manual stimulation (*left*). Each row of rasters is 1 presentation trial consisting of light cutaneous stimulation above the naris. Neural responses declined when temperature declined. (Note that in this pilot study, stimulus timing for each trial was imperfectly recorded by a coincident keyboard input; thus stimulus-response alignment is approximate.) At *right*, temperature data (gray trace) are shown with mean neural activity (black traces), temporally aligned to rasters. Solid black trace is driven activity during stimulation, and dotted black trace is spontaneous activity between stimuli; both are moving averages across trials during 10 s. Solid and dotted black lines below rasters at *left* mark the sampling windows for corresponding traces at *right*.

microelectrode/thermocouple ensemble following implantation. Chips were chronically implanted in rats, ferrets, and monkeys, and cortex was cooled in the weeks and months following chip implantation. Figure 12 shows cooling data obtained from these animals at different postimplantation days. As observed, the cortical temperature was successfully decreased and returned to normal. These results indicate that our chips are biocompatible and can maintain function over a period of months postimplantation. Histological examination of cortical tissue indicates that there was no cortical damage following chip implantation. Further information on chronic implantation must be presented separately.

Preliminary Tests of Magnetic Resonance Compatibility

A coil-design cooling chip plus microthermocouple were scanned with various objects to determine whether they caused distortions in the scanned image. In one scan, the cooling chip was attached to the surface of a phantom subject, a fluid-filled container approximating the geometry and MR properties of a human head. The microthermocouple extended several millimeters along the surface of the phantom. In another scan, the cooling chip was attached to an orange, and the microthermocouple was inserted several millimeters through the peel and into the fruit. Fruit is often used as a phantom in testing MR equipment because it has a recognizable internal structure observable in scans. It was especially useful for our test because we could easily insert a microthermocouple through the orange peel to test whether its presence inside the scanned object would lead to artifacts. The device plus thermocouple caused little or no distortion in the structural scans of the phantom subject or the orange (Fig. 13), suggesting that it would be possible to inactivate brain areas in animals during functional scans using our cooling device. Further tests of compatibility with functional MRI (fMRI) are ongoing.

DISCUSSION

This report describes the fabrication and implementation of an implantable, lightweight, highly flexible microfluidic cooling chip

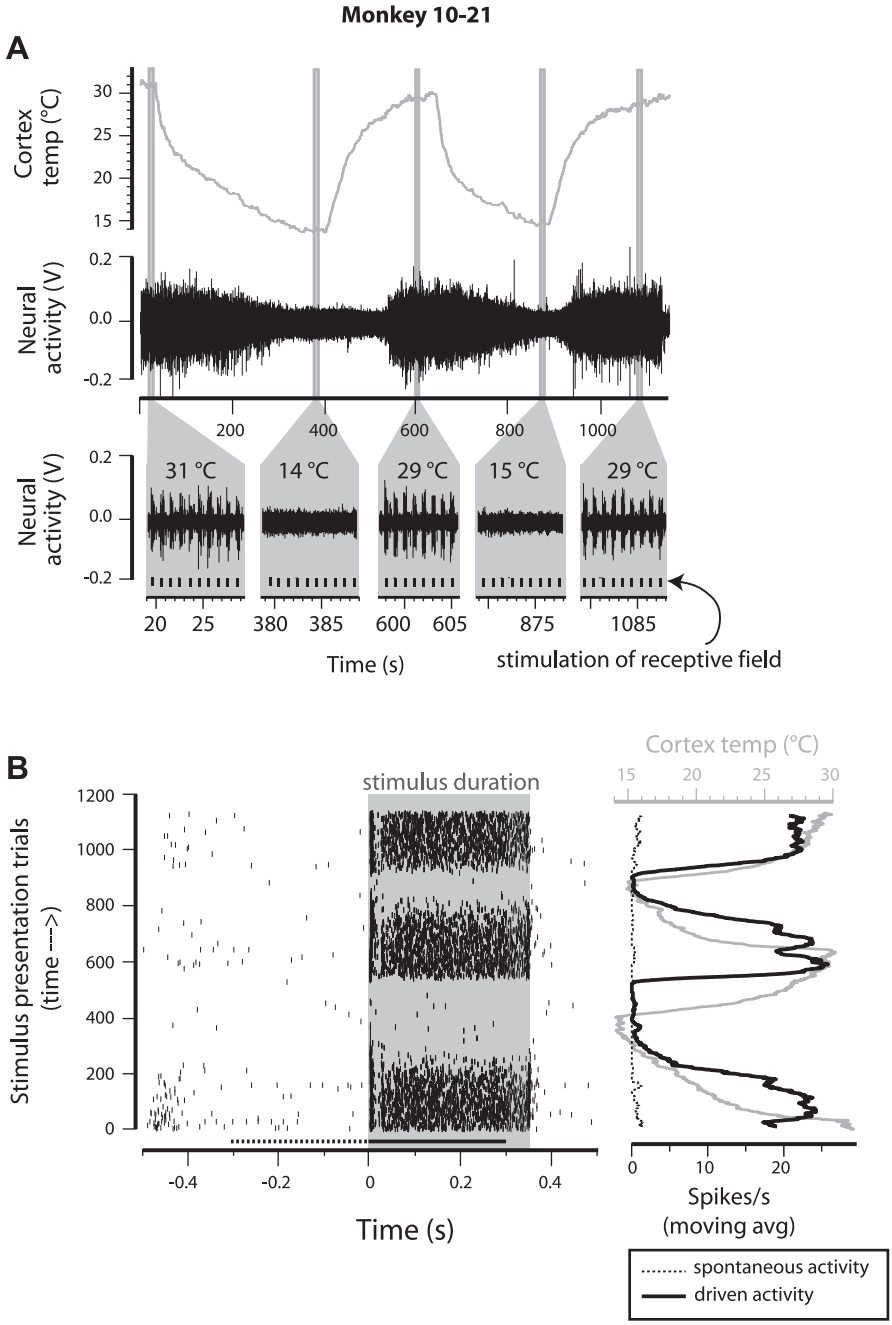

Fig. 11. Spontaneous and sensory-driven neural activity in area 1 of *monkey 10-21* during cooling. Details are similar to Fig. 10, except for the following. The receptive field on the hand of the monkey was stimulated by a stream of compressed air regulated by Spike2 software. Stimulus timing is therefore much more precisely known than for the study depicted in Fig. 10. The 1-Hz air puff had a duration of 300 ms and a pressure of ~20 lb/in^2.

that can reversibly deactivate neural function in a restricted region of the neocortex within minutes. We employed a control algorithm that uses thermal feedback from within cortex to automate coolant flow and allows precise maintenance of a target cortical temperature (Figs. 6*B* and 7). Target temperature was reached within minutes and was maintained within 0.3°C for an hour (Fig. 6*B*). This level of control allows one to vary the volume of the deactivated region precisely by changing the target temperature for the in-cortex microthermocouple.

We also observed the laminar and spatial spread of cooling under and around the chip. Cortical temperature was relatively uniform directly under the cooling chip (Fig. 6*A*), and cooling was restricted primarily to cortex under, rather than adjacent to, the cooling chip (Fig. 9). The spatial extent of deactivation can also be regulated with PDMS insulation, which was found to be effective for limiting cooling in one sulcal bank (Fig. 8).

As previous studies have showed (e.g., Antunes and Malmierca 2011; Coomber et al. 2011; Lomber et al. 1999), local cooling led to a rapid loss of neural activity that was restored within minutes of rewarming (Figs. 10 and 11). Cooling abolished sensory-driven neural responses and disrupted spontaneous activity in various ways. Driven neural activity and cortical temperature were tightly coupled, although our data show some delay. This may have been due to the electrode and microthermocouple tips having slightly different locations in cortex. Alternatively, neural activity may have been maintained until additional tissue deeper and farther lateral from the measurement point was affected, at which point the whole

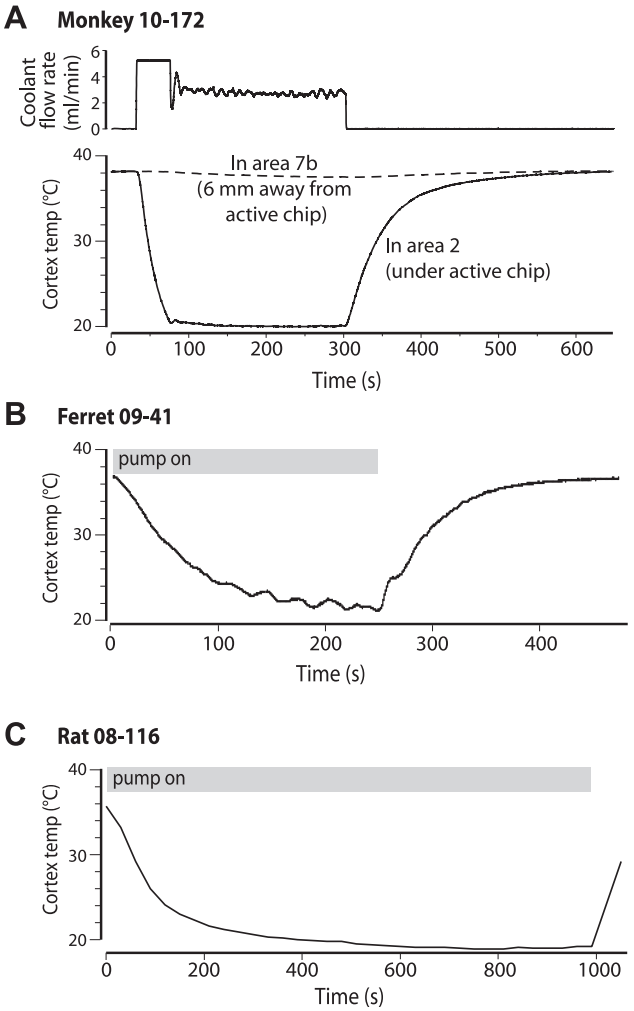

Fig. 12. Cooling of cortex following chronic implantation of cooling chip. *A*: 52 days postimplantation in *monkey 10-172*. *Top* trace is coolant pump speed. Dashed temperature trace is from microthermocouple in area 7b, 6 mm away from the active cooling chip. *B*: 15 days postimplantation in *ferret 09-41*. Gray box indicates cooling period. *C*: 4 days postimplantation in *rat 08-116*.

local network went silent. Observations of spontaneous activity may have been affected by similar factors. Under some circumstances, spontaneous activity was abolished (Fig. 11*B*) or reduced (Fig. 10*B*), whereas in others, spontaneous activity increased (data not shown). Increased spontaneous activity during cooling might be due to lateral inhibition with local reductions in neural activity causing increased activity in tissue close enough to affect the relatively low-impedance electrode used for multiunit recording. In addition, cooling alters a large number of factors affecting membrane properties and synaptic transmission, and one result, seen in slices of rat and cat cortical tissue, is that at intermediate temperatures, neurons are closer to spiking threshold and produce larger, longer duration spikes (Volgushev et al. 2000a, 2000b). It is difficult to know what these data, collected from slice tissue of uniform temperature, should predict about an in vivo preparation in which different parts of the neural network lie in different portions of a temperature gradient, each with different and sometimes opposing effects on spikes and synaptic behavior.

Cooling chips were tested successfully in rats, ferrets, and primates, a >50-fold range in brain size. By making minor adjustments in surgical techniques and cooling chip materials (particularly coolant tube diameter), this technique is scalable across a wide range of species types and sizes.

Our cooling chip has several important advantages over similar heat exchange devices. *1*) It is small (as small as 21 mm^3) and lightweight (0.16–0.5 g). *2*) Its adaptable design allows it to be used in animals as small as rats (even for chronic implantation) and to be altered to conform to the size and shape of a particular cortical field. *3*) It is easy to implant. *4*) Each chip contains one or two microthermocouples measuring cortical temperature. Electrodes can also be introduced near thermocouples to measure neural activity directly under the device. *5*) One side of the sulcal chip is insulated, restricting cooling to one sulcal bank. *6*) Cortical temperature is automatically regulated based on feedback from the in-cortex thermocouple. *7*) The small size of these cooling chips could allow for chronic implantation of multiple adjacent chips with independent feedback control. By activating different combinations of small, adjacent chips, a number of cortical areas can be deactivated in different combinations to assess the macrocircuitry underlying a number of complex abilities. *8*) Finally, we have provided specific instructions on how to fabricate and utilize the cooling device so that it can be disseminated beyond our own team of researchers.

Another advantage of our mostly nonmetallic design is the possibility that it can be adapted for fMRI to examine the hemodynamic response during reversible inactivation of restricted brain regions. Metal, particularly when ferromagnetic, can cause image artifacts and/or inductive heating. Preliminary tests suggest that our cooling chip, even when accompanied by a Cu-Ni microthermocouple, caused little or no distortion or artifact in acquired images (Fig. 13). Most equipment associated with our cooling setup can be located far from the animal and therefore does not need to be MR compatible. One exception is the dry ice

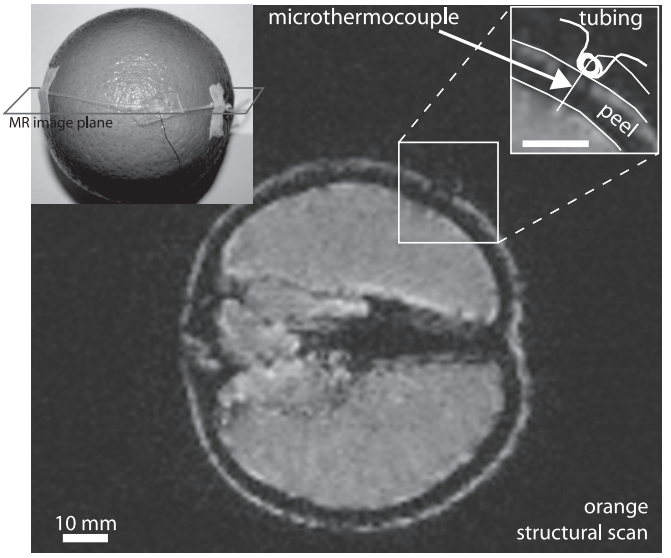

Fig. 13. Magnetic-resonance (MR) compatibility. MR compatibility was tested using a 3T Siemens (Erlangen, Germany) Trio scanner at the University of California, Davis Imaging Research Center. T1-weighted high-resolution anatomic images were acquired using an MP-RAGE (magnetization-prepared rapid-acquisition gradient-echo) sequence (repetition time, 2,500 ms; echo time, 4.32 ms; flip angle, 12°; matrix size, 256 × 256). A coil-design cooling device was secured to the surface of an orange. The fine metal thermocouple was positioned within the device, several millimeters into the orange. The coolant tubing was filled with gadolinium solution to aid visualization. The device plus thermocouple caused little or no distortion in the structural scans.

bath, which need contain no metal. The blunt, stainless steel syringe needle that couples the chip tubing to the cooling circuit can be substituted with a Teflon needle of similar configuration. Carbon fiber electrodes have been used successfully in MR-compatible electrophysiology at high field strengths (9.4 T; Dunn et al. 2009), opening the possibility of simultaneous thermal inactivation, functional imaging, and electrophysiological recording or electrical stimulation.

A primary application for the cooling chip in our laboratory will be to probe cortical macrocircuitry in monkeys and the specific behaviors that cortical areas generate. This device, however, can be adapted for number of neuroscience disciplines and animal models for studies of sensory, motor, and cognitive systems. Its user-friendly interface, with the use of commercially available hardware and software, will make it adaptable for use in many laboratories. Finally, issues such as neural basis of complex behaviors (currently conducted almost exclusively in nonhuman primates) that can be addressed more easily by rapid and reversible deactivation can now be addressed in the more ubiquitous rodent model.

ACKNOWLEDGMENTS

Jeffrey Padberg, Conor Weatherford, Jeffrey Johnson, and Arnold Chen also contributed to this work. We thank Adele Seelke for help with this manuscript.

Present address for A. Tiriac: Department of Psychology, University of Iowa, Iowa City, IA.

GRANTS

This work was supported by a McDonnell Foundation grant (to L. Krubitzer), National Science Foundation Faculty Early Career Development (CAREER) Award ECCS-0846502 (to T. Pan), and National Institutes of Health Grants NS35103 (to L. Krubitzer), NS59262 (D. F. Cooke), AI47294, and HL082689 (both to S. I. Simon).

DISCLOSURES

No conflicts of interest, financial or otherwise, are declared by the authors.

AUTHOR CONTRIBUTIONS

Author contributions: D.F.C., A.B.G., G.H.R., S.I.S., and L.K., conception and design of research; D.F.C., A.B.G., I.Y., A.T., G.H.R., and L.K. performed experiments; D.F.C., A.B.G., P.T., and A.T. analyzed data; D.F.C., A.B.G., G.H.R., S.I.S., and L.K. interpreted results of experiments; D.F.C., A.B.G., and L.K. prepared figures; D.F.C. and L.K. drafted the manuscript; D.F.C., A.B.G., P.T., G.H.R., T.P., S.I.S., and L.K. edited and revised the manuscript; D.F.C., A.B.G., and L.K. approved the final version of the manuscript.

REFERENCES

Alexander GE, Fuster JM. Effects of cooling prefrontal cortex on cell firing in the nucleus medialis dorsalis. *Brain Res* 61: 93–105, 1973.

Alvarado JC, Stanford TR, Vaughan JW, Stein BE. Cortex mediates multisensory but not unisensory integration in superior colliculus. *J Neurosci* 27: 12775–12786, 2007.

Antunes FM, Malmierca MS. Effect of auditory cortex deactivation on stimulus-specific adaptation in the medial geniculate body. *J Neurosci* 31: 17306–17316, 2011.

Aronov D, Fee MS. Analyzing the dynamics of brain circuits with temperature: design and implementation of a miniature thermoelectric device. *J Neurosci Methods* 197: 32–47, 2011.

Benita M, Conde H. Effects of local cooling upon conduction and synaptic transmission. *Brain Res* 36: 133–151, 1972.

Clarey JC, Tweedale R, Calford MB. Interhemispheric modulation of somatosensory receptive fields: evidence for plasticity in primary somatosensory cortex. *Cereb Cortex* 6: 196–206, 1996.

Clemo HR, Stein BE. Effects of cooling somatosensory cortex on response properties of tactile cells in the superior colliculus. *J Neurophysiol* 55: 1352–1368, 1986.

Coomber B, Edwards D, Jones SJ, Shackleton TM, Goldschmidt J, Wallace MN, Palmer AR. Cortical inactivation by cooling in small animals. *Front Syst Neurosci* 5: 53, 2011.

Dunn JF, Tuor UI, Kmech J, Young NA, Henderson AK, Jackson JC, Valentine PA, Teskey GC. Functional brain mapping at 9.4T using a new MRI-compatible electrode chronically implanted in rats. *Magn Reson Med* 61: 222–228, 2009.

Fuster JM, Alexander GE. Delayed response deficit by cryogenic depression of frontal cortex. *Brain Res* 20: 85–90, 1970.

Fuster JM, Bauer RH. Visual short-term memory deficit from hypothermia of frontal cortex. *Brain Res* 81: 393–400, 1974.

Girard P, Salin PA, Bullier J. Response selectivity of neurons in area MT of the macaque monkey during reversible inactivation of area V1. *J Neurophysiol* 67: 1437–1446, 1992.

Girard P, Salin PA, Bullier J. Visual activity in areas V3a and V3 during reversible inactivation of area V1 in the macaque monkey. *J Neurophysiol* 66: 1493–1503, 1991.

Horel JA. Perception, learning and identification studied with reversible suppression of cortical visual areas in monkeys. *Behav Brain Res* 76: 199–214, 1996.

Horel JA. Retrieval of active and inactive visual discriminations while temporal cortex is suppressed with cold. *Behav Brain Res* 51: 193–201, 1992.

Horel JA, Voytko ML, Salsbury KG. Visual learning suppressed by cooling the temporal pole. *Behav Neurosci* 98: 310–324, 1984.

Imoto H, Fujii M, Uchiyama J, Fujisawa H, Nakano K, Kunitsugu I, Nomura S, Saito T, Suzuki M. Use of a Peltier chip with a newly devised local brain-cooling system for neocortical seizures in the rat. *J Neurosurg* 104: 150–156, 2006.

Jiang W, Stein BE. Cortex controls multisensory depression in superior colliculus. *J Neurophysiol* 90: 2123–2135, 2003.

Krubitzer L, Huffman KJ, Disbrow E, Recanzone G. Organization of area 3a in macaque monkeys: contributions to the cortical phenotype. *J Comp Neurol* 471: 97–111, 2004.

Lomber SG. The advantages and limitations of permanent or reversible deactivation techniques in the assessment of neural function. *J Neurosci Methods* 86: 109–117, 1999.

Lomber SG, Malhotra S. Double dissociation of 'what' and 'where' processing in auditory cortex. *Nat Neurosci* 11: 609–616, 2008.

Lomber SG, Malhotra S, Sprague JM. Restoration of acoustic orienting into a cortically deaf hemifield by reversible deactivation of the contralesional superior colliculus: the acoustic "Sprague Effect". *J Neurophysiol* 97: 979–993, 2007.

Lomber SG, Payne BR. Task-specific reversal of visual hemineglect following bilateral reversible deactivation of posterior parietal cortex: a comparison with deactivation of the superior colliculus. *Vis Neurosci* 18: 487–499, 2001.

Lomber SG, Payne BR, Horel JA. The cryoloop: an adaptable reversible cooling deactivation method for behavioral or electrophysiological assessment of neural function. *J Neurosci Methods* 86: 179–194, 1999.

Long MA, Fee MS. Using temperature to analyse temporal dynamics in the songbird motor pathway. *Nature* 456: 189–194, 2008.

Malhotra S, Stecker GC, Middlebrooks JC, Lomber SG. Sound localization deficits during reversible deactivation of primary auditory cortex and/or the dorsal zone. *J Neurophysiol* 99: 1628–1642, 2008.

Malpeli JG. Reversible inactivation of subcortical sites by drug injection. *J Neurosci Methods* 86: 119–128, 1999.

Meredith MA, Kryklywy J, McMillan AJ, Malhotra S, Lum-Tai R, Lomber SG. Crossmodal reorganization in the early deaf switches sensory, but not behavioral roles of auditory cortex. *Proc Natl Acad Sci USA* 108: 8856–8861, 2011.

Michalski A, Wimborne BM, Henry GH. The effect of reversible cooling of cat's primary visual cortex on the responses of area 21a neurons. *J Physiol* 466: 133–156, 1993.

Michalski A, Wimborne BM, Henry GH. The role of ipsilateral and contralateral inputs from primary cortex in responses of area 21a neurons in cats. *Vis Neurosci* 11: 839–849, 1994.

Mishkin M. Analgous neural models for tactual and visual learning. *Neuropsychologia* 17: 139–151, 1979.

Mishkin M. A memory system in the monkey. *Philos Trans R Soc Lond B Biol Sci* 298: 85–95, 1982.

Mishkin M, Ungerleider LG. Contribution of striate inputs to the visuospatial functions of parieto-preoccipital cortex in monkeys. *Behav Brain Res* 6: 57–77, 1982.

Nakamoto KT, Jones SJ, Palmer AR. Descending projections from auditory cortex modulate sensitivity in the midbrain to cues for spatial position. *J Neurophysiol* 99: 2347–2356, 2008.

Nakamoto KT, Shackleton TM, Palmer AR. Responses in the inferior colliculus of the guinea pig to concurrent harmonic series and the effect of inactivation of descending controls. *J Neurophysiol* 103: 2050–2061, 2010.

Padberg J, Disbrow E, Krubitzer L. The organization and connections of anterior and posterior parietal cortex in titi monkeys: do New World monkeys have an area 2? *Cereb Cortex* 15: 1938–1963, 2005.

Padberg J, Franca JG, Cooke DF, Soares JG, Rosa MG, Fiorani M Jr, Gattass R, Krubitzer L. Parallel evolution of cortical areas involved in skilled hand use. *J Neurosci* 27: 10106–10115, 2007.

Padberg J, Recanzone G, Engle J, Cooke D, Goldring A, Krubitzer L. Lesions in posterior parietal area 5 in monkeys result in rapid behavioral and cortical plasticity. *J Neurosci* 30: 12918–12935, 2010.

Payne BR, Lomber SG. A method to assess the functional impact of cerebral connections on target populations of neurons. *J Neurosci Methods* 86: 195–208, 1999.

Ponce CR, Lomber SG, Born RT. Integrating motion and depth via parallel pathways. *Nat Neurosci* 11: 216–223, 2008.

Rushmore RJ, Valero-Cabre A, Lomber SG, Hilgetag CC, Payne BR. Functional circuitry underlying visual neglect. *Brain* 129: 1803–1821, 2006.

Sandell JH, Schiller PH. Effect of cooling area 18 on striate cortex cells in the squirrel monkey. *J Neurophysiol* 48: 38–48, 1982.

Schiller PH, Malpeli JG. The effect of striate cortex cooling on area 18 cells in the monkey. *Brain Res* 126: 366–369, 1977.

Seelke AM, Padberg JJ, Disbrow E, Purnell SM, Recanzone G, Krubitzer L. Topographic maps within Brodmann's area 5 of macaque monkeys. *Cereb Cortex* 2011.

Sherk H. Area 18 cell responses in cat during reversible inactivation of area 17. *J Neurophysiol* 41: 204–215, 1978.

Shindy WW, Posley KA, Fuster JM. Reversible deficit in haptic delay tasks from cooling prefrontal cortex. *Cereb Cortex* 4: 443–450, 1994.

Skinner JE, Lindsley DB. Reversible cryogenic blockade of neural function in the brain of unrestrained animals. *Science* 161: 595–597, 1968.

Tarnopolsky M, Seginer I. Leaf temperature error from heat conduction along thermocouple wires. *Agric For Meteorol* 93: 185–194, 1999.

Ungerleider LG, Mishkin M. Two cortical visual systems. In: *Analysis of Visual Behaviour*, edited by Ingle DJ, Goodale MA, Mansfield RJW. Cambridge: MIT Press, 1982, p. 549–586.

Volgushev M, Vidyasagar TR, Chistiakova M, Eysel UT. Synaptic transmission in the neocortex during reversible cooling. *Neuroscience* 98: 9–22, 2000a.

Volgushev M, Vidyasagar TR, Chistiakova M, Yousef T, Eysel UT. Membrane properties and spike generation in rat visual cortical cells during reversible cooling. *J Physiol* 522: 59–76, 2000b.

Zhang JX, Ni H, Harper RM. A miniaturized cryoprobe for functional neuronal blockade in freely moving animals. *J Neurosci Methods* 16: 79–87, 1986.